MECHANISM OF ACTION OF A BENZIMIDAZOLE SIRTUIN INHIBITOR, BZD9L1, IN COLORECTAL CANCER

TAN YI JER

UNIVERSITI SAINS MALAYSIA

2022

MECHANISM OF ACTION OF A BENZIMIDAZOLE SIRTUIN INHIBITOR, BZD9L1, IN COLORECTAL CANCER

by

TAN YI JER

Thesis submitted in fulfilment of the requirements
for the degree of
Doctor of Philosophy

August 2022

ACKNOWLEDGEMENT

The success of this project and completion of this dissertation have been made possible only through the guidance and support from various parties. To all whose names are not mentioned in this section, I thank you all the same and are ever grateful to your help and inspirations throughout my PhD journey.

First and foremost, I would like to thank my main supervisor Assoc. Prof. Dr Oon Chern Ein for her continuous guidance, patience, and support throughout the years. Her trust and dedication have allowed me to grow, excel, and matured into a proficient scientist. I would also like to thank my field supervisor Prof. Ricardo L Mancera for his willingness to provide me with the opportunity to explore the world of bioinformatics. His unwaning support during my stay in Australia and his expert knowledge in the field of structural biology definitely made my PhD journey more interesting and enjoyable. Special thanks also goes to Prof. Dr Gurjeet and Dr Sven Hans Petersen. Both of you are not only my mentors but are also good friends to me. My deep gratitude to the late Prof. Dr. Tan Soo Choon for his continued support throughout my adaptation period and during the commencement of the project, as well as providing me a platform for industrial exposure in the field of analytical chemistry. You will be deeply missed.

To my research mates, local and abroad, I would like you to know that it has been simply exceptional to get to know you. A big thanks to my lab partner Lee Yeuan Ting for sharing all the brainstorming, realization, and painstaking moments during the commencement of this project. All the hardships that we have surmounted together are no easy feat, and we will conquer more in the future! My appreciation also goes to my teammates in Malaysia (Dr Yeong Keng Yoon, Dr Ashwaq, Shandra, Cheng Wei Kang,

Ayappa Subramaniam, Mok Pei Yi, and Deepa Rajendran) and in Australia (Yvonne M Mukuka, Anji Babu Kapakayala, Christopher Malajczuk, Carlo Martinotti, John Tanner, Lanie Ruiz Perez, Phanendra Srikanth, Sandra Moore, Lina Rozano, and Krushna Sonar). I really enjoyed all the short chats, gatherings, and outings we have had. I would also like to thank all the administrative staff of INFORMM and the staff of USAINS Biomics Laboratory Testing Service Sdn Bhd for the support and assistance provided during my study. Special thanks to my partners in crime Mr Yeoh Seng Hoe and Dr Warren Lee for all the insightful comments, organizing chill outs from stresses, and providing me with immediate assistance whenever necessary.

I would like to acknowledge the Ministry of Higher Education Malaysia for Fundamental Research Grant Scheme (FRGS/1/2016/SKK15/USM/02/2) and Curtin University Training and Research Sponsorship (sponsorship ID no. 1990580481) for funding my project and my research attachment in Curtin Health Innovation Research Institute (CHIRI), Curtin University, Australia, respectively.

Most importantly, I must express my profound gratitude to my family and friends for their unfailing support and continuous encouragement. A personal thanks to my mum, dad, and my siblings for their inspirations, sacrifice, and unconditional love that have pushed me further and achieved higher than I can ever imagined. Also, to all my teachers from SJK(c) Gunung Rapat, Ipoh, Perak (primary education) and SMK Gunung Rapat, Ipoh, Perak (secondary education), as well as lecturers from Universiti Tunku Abdul Rahman, Kampar, Perak; thank you for instilling knowledge into me and shaping my character throughout these years. Last but not least, I would like to thank myself for being able to stay steadfast and remained passionate in research throughout the years. A very big thanks to all who had contributed to the success of this project.

TABLE OF CONTENTS

LIST OF TABLES

Page

LIST OF FIGURES

Page

LIST OF SYMBOLS AND ABBREVIATIONS

%	Percentage
~	Approximately
<	Less than
>	More than
$\times g$	Relative centrifugation force
≤	Less than or equal to
≥	More than or equal to
°C	Degree Celsius
µ	Micro- (unit of mass; e.g. µg, µL, µM)
1×	One time dilution
1° (Protein studies)	Primary antibody
2° (Protein studies)	Secondary antibody
5-FU	5-fluorouracil
ABC	ATP-binding cassette
ABCC	ATP binding cassette subfamily C
Akt	protein kinase B
ANOVA	Analysis of variance
APC	Adenomatous polyposis coli
Bad	BCL2 associated agonist of cell death
BAX	BCL2 associated X
BCL2	BCL2 apoptosis regulator
BIM	BCL2 like protein 11 (a.k.a. BCL2L11)
BRAF	Raf murine sarcoma viral oncogene homolog B
Casp	Caspase protein

CCS	Colorectal cancer subtypes
CD40	Tumour necrosis factor receptor superfamily member 5
Chk	Checkpoint kinase
CI	Combination index
c	Centi- (unit of mass; e.g. cm)
cm^2	Square centimeter
CO_2	Carbon dioxide
CRC	Colorectal cancer
CSL	CBF1, Suppressor of Hairless, Lag-1
CTNNB1	catenin beta 1
Cα RMSD	Structural backbone root-mean-square deviation
ddH_2O	Deionised water
dH_2O	Distilled water
DIABLO	Direct Inhibitor of Apoptosis-Binding protein with Low pI
DLL4	Delta like canonical Notch ligand 4
DP1	Transcription factor DP1
DR6	Death receptor 6
DS	Discovery Studio 4.0 software
E2F	transcription factor E2F
E-cadherin	Epithelial cadherin
EFGR	Epidermal growth factor receptor
eIF2-α	Eukaryotic initiation factor 2 alpha
Elk-1/SRF	ETS domain-containing protein Elk-1 associated with a dimer of serum response factor
EMT	Epithelial to mesenchymal transition
ERK1/2	Extracellular signal-regulated kinases 1 and 2
FBS	Foetal bovine serum

FCS	Functional class scoring
FDR	False discovery rate
g	Gram
GADD45A	Growth arrest and DNA damage inducible alpha
GAPDH	Glyceraldehyde-3-phosphate dehydrogenase
GO	Gene ontology
GOI	Genes of interest
GRIM-19	Retinoid-IFN-induced mortality-19
h	Hour(s)
H-bond	Hydrogen bond
HDC	High dose combination (25 μM BZD9L1 + 5 μM 5-FU)
HEY2	Hes related family bHLH transcription factor with YRPW motif 2
HEYL	Hes related family bHLH transcription factor with YRPW motif like
HSP27	Heat shock protein 27
HSP70	Heat shock protein 70
i.e.	*id est* (meaning "that is")
IDH1	Isocitrate dehydrogenase 1
IGFBP	Insulin like growth factor binding protein
IgG	Immunoglobulin G
IgG (H+L)	Heavy chain and light chain of immunoglobulin G
IQGAP1	IQ motif containing GTPase activating protein 1
ITGA5	Integrin subunit alpha 5
IκBα	Nuclear factor of kappa light polypeptide gene enhancer in B cells inhibitor alpha
JAG1	Jagged canonical Notch ligand 1
k	Kilo- (unit of mass; e.g. kg)

Ki67	Antigen Ki67
KRAS	Kirsten rat sarcoma 2 viral oncogene homolog
L	Litre
LDC	Low dose combination (10 μM BZD9L1 + 5 μM 5-FU)
M	Molar
mAb	Monoclonal antibody
Max	Myc associated factor X
MDR1	Multidrug resistant gene 1
m	Mili- (unit of mass; e.g. mg, mL, mM)
min	Minute(s)
mm^3	Cubic milimeter
MMP9	Matrix metallopeptidase 9
MRP	Multidrug resistant associated protein
MSI	Microsatellite instable
MSS	Microsatellite stable
MTT	3-(4,5-dimethylthiazol-2-yl)-2,5-diphenyl tetrazolium bromide
Myc	Myc proto-oncogene, bHLH transcription factor
N_2	Nitrogen
NAD+	Nicotinamide adenine dinucleotide
NFκB	Nuclear factor kappa-light-chain enhancer of activated B cells
n	Nano- (unit of mass; e.g. ng, nm, nM)
NICD	Notch intracellular domain
NSF	Non-spheroids forming
ORA	Target over-representation analysis
OS	Overall survival
p21	Cyclin-dependent kinase inhibitor 1A

p38 MAPK	p38 mitogen-activating protein kinase
p53	Tumour protein p53
PA	Pathway analysis
pAb	Polyclonal antibody
PARP	Poly(ADP-ribose)polymerase
PBS	Phosphate buffer saline
PDB	RCSB Protein Data Bank
PFS	Progression-free survival
pH	Scale used to measure acidity/alkalinity of a solution
PIG3	p53-inducible gene 3
PIK3CA	Phosphatidylinositol-4,5-bisphosphate 3-kinase catalytic subunit alpha
PPI	Protein-protein interaction
pRB	Retinoblastoma protein
PTEN	Phosphatase and tensin homolog
PUMA	p53 upregulated modulator of apoptosis
RBP-Jk	Recombining signal binding protein for immunoglobulin kappa J region
RCTs	BZD9L1-regulated candidate targets
RFS	Relapse-free survival
ROS	Reactive oxygen species
SAPK/JNK	Stress-activated protein kinase/c-Jun NH(2)-terminal kinase
SA-β-gal	Senescence-associated beta-Galactosidase
SCRIB	Scribble planar cell polarity protein
sec	Second(s)
SEM	Standard error of the mean
SIRT	Sirtuin

SIRT4_SM	Human SIRT4 homology models were generated using SWISS-MODEL server
SIRT7_SM	Human SIRT7 homology models were generated using SWISS-MODEL server
SMAC	Second mitochondria-derived activator of caspase
Smad	Mothers against decapentaplegic
SNAI	Snail family transcriptional repressor
STAT3	Signal transducer and activator of transcription 3
sTNF-R1	Soluble tumour necrosis factor receptor 1
Survivin	Baculoviral inhibitor of apoptosis repeat-containing protein 5 (a.k.a. BIRC5)
TAK1	Transforming growth factor-β activated kinase-1
TGF-β1	Transforming growth factor beta 1
TNF-α	Tumour necrosis factor alpha
TRAF2	TNF receptor associated factor 2
Twist	Twist protein
V	Voltage
v/v	Volume per volume
Vimentin	Fibroblast intermediate filament
Vina	AutoDock Vina
w/v	Weight per volume
ZEB1	Zinc finger E-box binding homeobox 1
β-actin	Beta-actin
ΔΔCT	Comparative cycle number at the threshold level of log-based fluorescence method
-ΔG	Ligand binding free energy values

LIST OF APPENDICES

of active-site residues. Residues with asterisk (*) were non-preselected active site residues used for docking with flexible side chains. Interactions were visualized and determined using Discovery Studio 4.0 software.

Appendix 3.1 The purity of synthesized BZD9L1 was assessed using HPLC-DAD. Chromatogram with overlapped peaks along the spectra (wavelength = 254, 280, 315, 342, and 365 nm) for DAD and fluorescent detector (excitation/emission = 346 nm/448 nm) indicates that BZD9L1 is pure (red box). The peak areas of BZD9L1 for each wavelength was > 90% mAU in DAD, indicating > 90% purity. Analysis was performed using the Agilent Technologies 1260 Infinity II LC System and Agilent Chemstation software. Column, Agilent Poreshell 120 EC-C18 (4.6 × 150mm, i.d.,4 µM); column temperature, 25 °C; mobile phase, methanol: water (75:25); flow rate, 1.0 mL/min. A concentration of 100 µg/mL BZD9L1 in methanol was used for analysis.

Appendix 3.2 QPCR analysis showed **(a)** 25 µM BZD9L1 treatment caused upregulation of DLL4, HEY2 and HEYL, and downregulation of JAG1 gene expression levels in HCT 116 cells at 24 h. **(b)** KEGG pathway analysis revealed that BZD9L1 induced the activation of the Notch signalling pathway in HCT 116 cells. Nodes labelled green indicate upregulation and nodes labelled pink indicate downregulation. Statistical analysis (*$p<0.05$, **$p<0.01$, ***$p<0.001$, ****$p<0.0001$, Student's t-test, n = 3 independent experiments) was done using GraphPad Prism 6.0. Error bars represent standard error of the mean.

Appendix 3.3 Gene Ontology (GO) function and enrichment analysis of total BZD9L1-regulated candidate targets (RCTs) on **(a)** biological process, **(b)** molecular function and **(c)** cellular component using PANTHER GO-slim modules from PANTHER Classification System database version 14.1. Statistical analysis (* indicates p-value < 0.05, # indicates FDR < 0.05, Fisher's exact test) performed using internal tools from PANTHER database.

Appendix 3.4 Gene Ontology (GO) function and enrichment analysis of upregulated BZD9L1-regulated candidate targets (RCTs) on **(a)** biological process, **(b)** molecular function and **(c)** cellular component using PANTHER GO-slim modules from PANTHER Classification System database version 14.1. Statistical analysis (* indicates p-value < 0.05, # indicates FDR < 0.05, Fisher's exact test) performed using internal tools from PANTHER database.

Appendix 3.5 Gene Ontology (GO) function and enrichment analysis of downregulated BZD9L1-regulated candidate targets (RCTs) on **(a)** biological process, **(b)** molecular function and **(c)**

MEKANISME TINDAKAN PERENCAT SIRTUIN BENZIMIDAZOLE, BZD9L1, DALAM KANSER KOLOREKTAL

ABSTRAK

Sirtuins (SIRT) adalah deasetilase yang bergantung pada NAD^+ dan terlibat dalam pelbagai penyakit epigenetik termasuk penyakit kardiovaskular dan neurodegeneratif, diabetes, penuaan dan barah. Kemunculan SIRT sebagai sasaran terapi dan keterbatasan perencat SIRT yang sedia ada membawa kepada penemuan perencat SIRT baharu: BZD9L1. Oleh sebab pengujian kesan BZD9L1 pada aktiviti enzim SIRT terhalang atas kebolehsediaan kit komersil, interaksi BZD9L1 pada SIRT dikaji menggunakan pemodelan molekul dan kajian dok. Kajian dok molekul mendedahkan bahawa BZD9L1 mungkin mengikat SIRT1-3, 6 dan 7 dengan pengesahan yang serupa tetapi dengan pertalian yang berbeza, dengan itu mengembangkan potensi terapi BZD9L1 dalam penyakit metabolik. Di samping itu, pendekatan *in silico* telah digunakan untuk menjelaskan mekanisme termodulasi BZD9L1 berdasarkan data eksperimen sedia ada . Analisis *in silico* sasaran terkawal BZD9L1 menunjukkan bahawa percambahan dan apoptosis sel HCT 116 mungkin disebabkan oleh laluan isyarat yang bergantung pada p53. BZD9L1 didapati berkesan terhadap titisan sel barah yang berbeza terutamanya barah kolorektal (CRC), di mana rejimen kemoterapi baris pertama 5-fluorouracil (5-FU) sering mengakibatkan kegagalan rawatan akibat ketidakpekaan dadah dan kesan sampingan yang teruk. Memandangkan usaha semasa untuk mengatasi batas-batas ini melibatkan pemekaan tumor melalui rawatan adjuvan, projek ini juga bertujuan untuk memberikan pandangan baharu tentang potensi pembangunan BZD9L1 sebagai adjuvan kepada 5-FU dalam terapi CRC menggunakan model *in vitro* dan *in vivo*. Gabungan BZD9L1 dan 5-FU didapati lebih berkesan terhadap titisan sel HCT 116 CRC dalam mengurangkan daya

maju dan kemandirian sel berbandingrawatan tunggal melalui kesan sinergi. Rawatan gabungan juga meningkatkan apoptosis, menyebabkan terhenti kitaran sel fasa-S, menyebabkan penuaan, dan kekerapan mikronukleus berbanding dengan rawatan tunggal dalam sel HCT 116. Selain itu, rawatan gabungan lebih berkesan mencetuskan apoptosis dan mengurangkan penghijrahan sferoid HCT 116. Rawatan kedua-dua BZD9L1 dan 5-FU menunjukkan pengurangan kadar pertumbuhan tumor HCT 116 tetapi tidak menyebabkan perubahan berat badan *in vivo*, menonjolkan kesan terapeutik rejim rawatan gabungan.

MECHANISM OF ACTION OF A BENZIMIDAZOLE SIRTUIN INHIBITOR, BZD9L1, IN COLORECTAL CANCER

ABSTRACT

Sirtuins (SIRTs) are NAD+-dependent deacetylases that is implicated in various epigenetic diseases including cardiovascular and neurodegenerative diseases, diabetes, aging and cancer. The emergence of SIRTs as therapeutic targets and limitations of existing SIRT inhibitors led to the discovery of a novel SIRT inhibitor: BZD9L1. As testing of the effects of BZD9L1 on the enzymatic activities of SIRTs have been hampered by the availability of commercial kits, BZD9L1 interactions on SIRTs were studied using molecular modelling and docking studies. Molecular docking studies revealed that BZD9L1 may bind to SIRT1-3, 6 and 7 with similar confirmation but with different affinities, thereby expanding the therapeutic potential of BZD9L1 in metabolic diseases. In addition, *in silico* approaches were deployed to further elucidate BZD9L1-modulated mechanisms based on existing experimental data. In silico analysis of BZD9L1-regulated targets showed that the proliferation and apoptosis of HCT 116 cells may be due to p53-dependent signalling pathways. BZD9L1 was found to be effective against different cancer cell lines especially colorectal cancer (CRC), where its first-line chemotherapy regimen 5-fluorouracil (5-FU) often result in treatment failure due to drug insensitivity and severe side effects. As current efforts to overcome these boundaries involved sensitizing tumours through adjuvant treatments, this project also aims to provide novel insights into the potential development of BZD9L1 as an adjuvant to 5-FU in CRC therapy using *in vitro* and *in vivo* models. The combination of BZD9L1 and 5-FU was found to be more effective against HCT 116 CRC cell line in reducing cell viability and survival compared to sole treatment via synergistic effect. Combined treatments also increased apoptosis, induced S-phase cell cycle arrest, induced

senescence and frequency of micronucleus compared to sole treatments in HCT 116 cells. Moreover, combined treatments more effectively triggered apoptosis and reduced migration of HCT 116 spheroids. Treatment of both BZD9L1 and 5-FU showed reduced growth rate of HCT 116 tumours but did not cause body weight change *in vivo*, highlighting the therapeutic effects of combined treatment regimes.

CHAPTER ONE

INTRODUCTION AND LITERATURE REVIEW

1.1 Colorectal cancer

Colorectal cancer (CRC) is the cancer of the colon and the rectum that arises from malignant polyps, which are abnormal outgrowths within the inner lining of the large intestinal wall (Amersi et al., 2005; Aarons et al., 2014). CRC is ranked as the third most common malignancy globally and is among the most common cancers in developing countries (Globocan, 2020; Sung et al., 2021). In the year 2020 alone, a total of 1,931,590 CRC incidences (10.0% of all cancer cases) with 915,880 recorded mortalities (576,858 cases for colon cancer and 339,022 cases for rectum cancer) were recorded (Globocan, 2020). Although the worldwide CRC mortality rate has been decreasing in recent years, the escalating CRC incidence rate in most countries continued to contribute to the global cancer burden despite medical advancement (Safiri et al., 2019). Furthermore, among all cancers, the incidence of CRC is the third and second highest among all male and female cancer cases, respectively (Sung et al., 2021).

In Malaysia, CRC is the second most common cancer with 3,540 recorded incidences (2,035 cases for colon cancer and 1,385 cases for rectum cancer) and 320 reported mortality in the year 2020 alone (Globocan, 2020). According to the Malaysian National Cancer Registry, the five-year survival rate among Malaysian male and female CRC patients was merely 49.0% and 53.8%, respectively, due to delayed prognosis (National Cancer Registry, 2018). Moreover, approximately 65.0% of CRC patients were diagnosed in the later stages (stage III and stage IV) at the time

of diagnosis (Arunah Chandran et al., 2020). The prevalence of CRC has thus posed an onerous challenge for local and global healthcare sectors to develop more efficient therapeutic options to further improve CRC treatment efficacies and increase CRC patients' overall survival (OS) rate.

1.1.1 Classification and staging of CRC

CRC can be staged based on the traditional Duke's classification system or the more recent American Joint Committee on Cancer (AJCC) tumour-node-metastasis (TNM) classification and staging system. In Duke's classification system, CRC can be divided into three stages (Stage A, B, and C) based on tumour localization. Patients were categorized as Stage A when tumours are confined at the intestinal/rectal wall, Stage B when tumours invaded the smooth muscles, and Stage C when malignant cells metastasized into the lymph nodes (Sarma, 1986). However, this classification was later modified to Dukes' A, Dukes' B, Dukes' C and Duke's D based on tumour localization at the mucosa, muscularis propria, invaded to at least one lymph node, and widespread metastasis, respectively (Akkoca et al., 2014). Compared to the TNM classification system, Duke's system is outdated and is not recommended for modern clinical practice.

The TNM classification and staging system for CRC can be divided into four main stages (Stage I-IV) with differently characterized prognostic and therapeutic outcomes. This system was designed based on the characteristics of the primary tumour (T) and the extent of regional lymph node involvement (N) and distant metastasis (M) (Sagaert et al., 2018; Weiser, 2018). The different categories used for CRC staging based on the TNM system are outlined in Table 1.1.

Table 1.1 Staging of CRC based on the TNM classification system.

Stage	Tumour (T)	Node (N)	Metastasis (M)
0	Tis	N0	M0
I	T1 or T2	N0	M0
IIA	T3	N0	M0
IIB	T4a	N0	M0
IIC	T4b	N0	M0
IIIA	T1 or T2	N1/ N1c	M0
	T1	N2a	M0
IIIB	T3 or T4	N1/ N1c	M0
	T1 or T2	N2b	M0
IIIC	T4	N2a	M0
	T3 or T4	N2b	M0
	T4b	N1 or N2	M0
IVA	Any T	Any M	M1a
IVB	Any T	Any M	M1b
IVC	Any T	Any M	M1c

Key for TNM Staging:

Primary Tumour (T)

Tis: Carcinoma *in situ*.

T1: Tumour in the inner layer of the bowel.

T2: Tumour has grown into the muscle layer of the bowel wall.

T3: Tumour has grown into the outer lining of the bowel wall but has not grown through it.

T4a: Tumour has grown through the outer lining of the bowel wall and has spread into the tissue layer (peritoneum) covering the organs in the tummy (abdomen).

T4b: Tumour has grown through the bowel wall into nearby organs.

Regional Lymph Nodes (N)

N0: No spread to lymph nodes.

N1a: Spread to 1 lymph nodes.

N1b: Spread to 2 or 3 lymph nodes.

N1c: Nearby lymph nodes don't contain cancer, but there are cancer cells in the tissue near the tumour.

N2a: Spread to 4-6 lymph nodes.

N2b: Spread to >7 lymph nodes.

Distant Metastases (M)

M0: No metastasis.

M1a: Cancer has spread to 1 distant site or organ.

M1b: Cancer has spread to 2 or more distant sites or organs.

M1c: Cancer spread to distant organs and peritoneum.

1.1.2 Epigenetic regulation and heterogeneity of CRC

CRC tumours are usually made up of a heterogenous group of malignant cells with distinct origins. Although about 90% of CRC are adenocarcinomas derived from the epithelial lining of the colon (Fleming et al., 2012), CRC can also develop from adenosquamous cells, neuroendocrine cells, squamous cells, signet ring cells, spindle cells and undifferentiated carcinoma cells (Fleming et al., 2012; Hahn et al., 2016). The transformation of CRC adenomas and carcinomas from normal glandular colon epithelial cells may be attributed to the accumulation of genetic and epigenetic mutations, which are also sporadic and found in approximately 80% of CRC incidents (Fearon, 2011; Ewing et al., 2014). Alterations of these cancer driver genes are consequences of chromosomal instability, defective DNA repair mechanism, and inappropriate methylator/CpG island methylation phenotype (dos Santos et al., 2019; Sagaert et al., 2018). Tumour heterogeneity remains a major challenge in cancer therapeutics due to its negative correlation with prognosis and treatment efficacy. The heterogeneity of CRC is subdivided into inter-patient heterogeneity and intra-tumour heterogeneity, where the latter can also be further classified into inter-metastatic heterogeneity and spatial heterogeneity (Molinari et al., 2018; Sagaert et al., 2018). According to Sveen and colleagues, the intra-patient and inter-metastatic heterogeneity are strong prognostic determinants. Their study revealed that patients with a lower level of heterogeneity exhibited a higher progression-free survival (PFS) and OS rate compared with those harbouring tumours of higher heterogeneity (Sveen et al., 2016).

The heterogeneity of CRC is tightly linked to the epigenetic regulation of an independent consortium of gene sets. Analysis on the mutation profile of CRCs revealed that TP53, KRAS, APC, PIK3CA, FBXW7, TCF7L2, SMAD4, and NRAS

are among the driver genes of non-hypermutated CRC; whereas BRAF, APC, MSH3, MSH6, CVR2A, TGFBR2, SLC9A9, TCF7L2, and KRAS are the common drivers found in hypermutated CRC tumours (Cancer Genome Atlas Network, 2012; Zehir et al., 2017; Dienstmann et al., 2018; Priestley et al., 2019; dos Santos et al., 2019). In metastatic CRC, targets such as APC, TP53, KRAS, and PIK3CA are essential recurrent genes that drive disease progression (Dienstmann et al., 2018). The presence of distinguished gene sets associated with individual CRC phenotypes thus highlights the heterogeneity of CRC that further complicates therapeutic options.

CRC can be classified into three main colorectal cancer subtypes (CCS): CCS1, CCS2 and CCS3 (De Sousa E Melo et al., 2013). Among all cases of CRC, the CCS1, CCS2, and CCS3 subtypes consist of 49%, 24%, and 27% total incidence, respectively. Tumours of the CCS1 subtype are localized at the distal colon, are chromosomal-instable (CIN), and encompasses mutated KRAS and/or TP53 genes. Commonly localized at the proximal colon, the CCS2 subtype demonstrates microsatellite instability (MSI) and exhibits CpG island methylator phenotype (CIMP). For CRC tumours expressing the CCS3 subtype, the heterogenous cell mass will exhibit both microsatellite stable/instable (MSS/MSI) and CIMP status, demonstrate BRAF and KRAS mutations, and are evenly distributed throughout the colon (De Sousa E Melo et al., 2013). On the other hand, the Consensus Molecular Subtype (CMS) classification system categorized CRC tumours into four main subtypes: CMS1, CMS2, CMS3, and CMS4 with varied gene expressions and pathological characteristics (Guinney et al., 2015). The CMS1 subtype of CRC is the MSI immune subtype and possess characteristics of high BRAF mutation, hypermutated, unstable microsatellite, and is associated with strong immune activation. The CMS2 subtype is also known as the canonical subtype that exhibits epithelial differentiation with

marked WNT and MYC signalling activation. The CMS3 subtype is the metabolic subtype of CRC which refers to epithelial CRC with enriched metabolic dysregulation encompassing KRAS mutation, whereas the CMS4 mesenchymal subtype exhibit gene signatures involved in the epithelial mesenchymal transition (EMT), TGF-β signalling pathway activation, stromal invasion, and angiogenesis (Guinney et al., 2015). Collectively, the heterogeneity of CRC subtypes may be attributed to the alteration of cancer pathways (MSI, CIN and CIMP), central gene mutations (e.g. KRAS, BRAF and p53), and varied gene expressions (Wang et al., 2019). Although the identification of CRC subtypes may better customize therapeutic options towards CRC patients, the heterogeneity of CRC tumours necessitates further elucidation of predictive biomarkers and better treatments. The lack of effective molecular therapy strategies, especially for advanced stages of CRC, also warrants the continuous development and discovery of novel targeted therapy candidates.

1.1.3 Mutation profile of HCT 116, HT-29, LIM1215 and Caco-2 CRC cell lines

Although a wide array of CRC cell lines was isolated and are currently used for research and development, some of the commonly employed CRC cell lines are the HCT 116, HT-29, LIM1215, and Caco-2. Based on information extracted from ATCC, the Expasy website, and reports by others (Ahmed et al., 2013; Berg et al., 2017; Fichtner et al., 2020), the different mutation profiles harboured by these cell lines are presented in Table 1.2.

Table 1.2 Mutation profile of HCT 116, HT-29, LIM1215, and Caco-2 colorectal cancer cell lines.

Cell lines/ Genes	HCT 116	HT-29	LIM1215	Caco-2
Disease	Carcinoma	Adenocarcinoma	Carcinoma	Adenocarcinoma
Tissue	Colon	Colon	Omental metastasis	Colon
Stage	IV	III	IV	-
MSI/MSS status	MSI	MSS	MSI	MSS
CIN status	negative	positive	-	positive
CMS status	CMS1, CMS4	CMS1, CMS3	CMS2	CMS4
PTEN	Positive	Positive	Positive	Positive
KRAS	G13D	wt	wt	wt
TP53	wt	R273H	wt	E204X
BRAF	wt	V600E	wt	wt
PIK3CA	H1047R	wt	H1047R	wt

Abbreviations: CIN, chromosomal instability pathway; CMS: consensus molecular subtypes MSI, microsatellite instability; MSS, microsatellite stable; wt, wild type.

1.2 CRC therapy and management

The five-year survival rate of CRC patients is highly dependent on the tumour stage upon diagnosis, in which patients diagnosed with localized tumours possessed a higher survival rate (~90%) compared to late-stage metastatic patients (~10%) (Brenner and Chen, 2018). Generally, the five-year survival rate of CRC patients decreases as the malignancy progresses along the stages. Patients harbouring the initial stage with localized colorectal tumours possessed a 5-year survival rate of 94.0%. In contrast, patients diagnosed with stage II and stage III CRC may experience a lower five-year survival rate of 82.0% and 67%, respectively. However, patients with stage IV or metastatic CRC will only have a five-year survival rate of 11.0%, thus emphasizing the importance of early detection (Sagaert et al., 2018; Xie et al., 2020). Diagnosis of CRC at the early stage is often challenging due to the lack of specific symptoms, which frequently lead to delayed prognosis (Vega et al., 2015). According to the Cancer Genome Atlas Network, approximately 30% of total CRC patients were diagnosed at an advanced stage with metastatic diffusion. In comparison, the remaining 20% of patients eventually developed metachronous metastases after undergoing standard treatments (Cancer Genome Atlas Network, 2012).

For most CRC cases, the initial treatment involves minimally invasive surgery for the removal of localized tumours (Babaei et al., 2016; Brenner and Chen, 2018). Surgical therapy is also commonly supplemented with neoadjuvant radiotherapy for the treatment of stage II and stage III rectal cancer (Brenner et al., 2014; Babaei et al., 2018b). However, surgery is usually combined with adjuvant chemotherapy for the management of high-risk stage II, stage III, and stage IV colon cancer patients (Brenner et al., 2014; Babaei et al., 2018a). Patients with stage IV rectal cancer are usually treated via surgical bypass of local bowel obstruction coupled with localized

chemoradiation for palliative purposes. In contrast, the therapeutic approach for stage IV colon cancer involves surgical resection, metastasectomy, and colectomy (Carethers, 2008a; Sagaert et al., 2018).

To date, an array of FDA-approved drugs was used either as a single treatment or as an adjuvant for combination treatments in CRC therapy (Table 1.3). Some of the most used compounds for CRC treatment consisted of conventional chemotherapy drugs and targeted therapy drugs, e.g., 5-fluorouracil (5-FU), Panitumumab, Oxaliplatin, Capecitabine, Irinotecan, Bevacizumab, and Cetuximab. Nevertheless, 5-FU has remained a mainstay as the first-line regimen for CRC treatment despite being a conventional chemotherapy compound (Hirsh and Zafar, 2011).

Table 1.3 FDA-approved drugs used for the treatment of CRC.

Treatment type	Compound(s) (***Brand name***)
Single-agent standard chemotherapy	Fluorouracil (5-FU), Capecitabine (*Xeloda*), Leucovorin calcium, Oxaliplatin (*Eloxatin*), Trifluridine and Tipiracil hydrochloride (*Lonsurf*)
Single-agent targeted therapy	Bevacizumab (*Avastin*, *Alymsys*, *Mvasi*, *Zirabev*), Cetuximab (*Erbitux*), Irinotecan hydrochloride (*Camptosar*), Ipilimumab (*Yervoy*), Nivolumab (*Opdivo*), Panitumumab (*Vectibix*), Pembrolizumab (*Keytruda*), Ramucirumab (Cyramza), Regorafenib (*Stivarga*), Ziv-Aflibercept (*Zaltrap*)
Combination treatment regime	CAPOX (Capecitabine + Oxaliplatin), FOLFIRI (Leucovorin calcium + Fluorouracil + Irinotecan hydrochloride), FOLFIRI-BEVACIZUMAB (Leucovorin calcium + Fluorouracil + Irinotecan hydrochloride + Bevacizumab), FOLFIRI-CETUXIMAB (Leucovorin calcium + Fluorouracil + Irinotecan hydrochloride + Cetuximab), FOLFOX (Leucovorin calcium + Fluorouracil + Oxaliplatin), FU-LV (Fluorouracil + Leucovorin calcium), XELIRI (Capecitabine + Irinotecan hydrochloride), XELOX (Capecitabine + Oxaliplatin)

Abbreviations: FDA, U.S. Food and Drug Administration; CRC, colorectal cancer.

1.2.1 The chemotherapy agent: 5-FU

Ever since its clinical introduction in the 1950s, both 5-FU and its oral prodrug capecitabine have been the first-line chemotherapeutic option for palliative and adjuvant treatment of CRC (Healey et al., 2013; Cho et al., 2020). The chemotherapy agent 5-FU was known to exert its anticancer effects by crippling the thymidylate synthase (TS), as well as incorporating its metabolites into the RNA and DNA strands during the elongation process of the cell cycle (Longley et al., 2003; Sethy and Kundu, 2021).

Upon activation, 5-FU is converted into three main active metabolites: fluorodeoxyuridine monophosphate (FdUMP), fluorodeoxyuridine triphosphate (FdUTP) and fluorouridine triphosphate (FUTP). The FdUMP was reported to bind TS and form a stable ternary complex with 5,10-methylenetetrahydrofolate, which may in turn inhibit dTMP synthesis via blocking proper dUMP substrate binding to the enzyme (Longley et al., 2003). The inhibition of TS will also result in the disruption of the deoxynucleotide pool (dATP/dTTP ratio), which may increase deoxyuridine triphosphate (dUTP) levels and cause impairment of the DNA synthesis and repair mechanisms (Longley et al., 2003). Furthermore, the misincorporation of FDUTP into the DNA and FUTP into RNA, respectively, may also disrupt normal DNA and RNA processing and function; which can lead to profound effects on the cellular metabolism and cell viability (Longley et al., 2003).

However, 5-FU standalone treatment may possess several limitations, such as reduced efficacy toward late-stage CRC (10-15% in stage III resected CRC), short-lived therapeutic effects, drug resistance, and susceptibility to post-treatment tumour recurrence (Healey et al., 2013; Cho et al., 2020; Sethy and Kundu, 2021). These shortcomings have thus emphasized the development of 5-FU as an adjuvant to be

combined with other agents, including the standard chemotherapy drugs leucovorin and oxaliplatin, to target late-stage colon cancer (Haller et al., 2005; Twelves et al., 2005; Sethy and Kundu, 2021).

1.2.2 Molecular targeted therapy

1.2.2(a) Targeting cancer hallmarks

Tumorous cells typically develop hallmark traits upon malignant transformation by growing against normal regulatory mechanisms. The most recently proposed 'Hallmarks of Cancer, circa 2022' comprises ten cancer hallmarks, two emerging hallmarks, and two enabling characteristics that may be manifested by human cells in the journey from normalcy to neoplastic growth states (Hanahan, 2022). As shown in Figure 1.1, the established cancer hallmarks are evading growth suppressors, avoiding immune destruction, enabling replicative immortality, tumour-promoting inflammation, activating invasion and migration, inducing vasculature, genome instability and mutation, resisting cell death, deregulating cellular metabolism, and sustaining proliferative signalling; the emerging hallmarks are senescent cells and unlocking phenotypic plasticity; and the enabling characteristics are non-mutational epigenetic reprogramming and polymorphic microbiome (Hanahan, 2022; Licciulli, 2022). In cancer therapeutics, targeted therapy agents aim to control malignancy via inhibition of these aberrant hallmark changes in the tumorous cells (Siddiqa and Marciniak, 2008; Al-Bedeary et al., 2020).

(a)

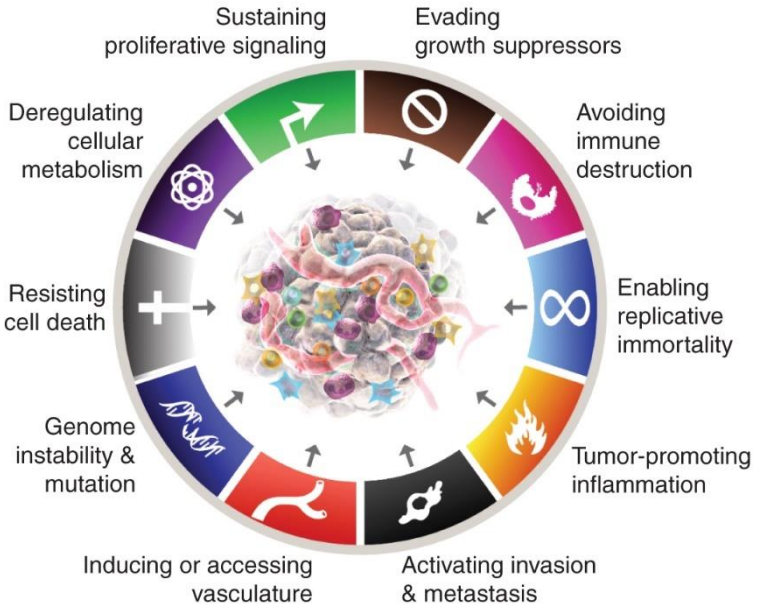

(b)

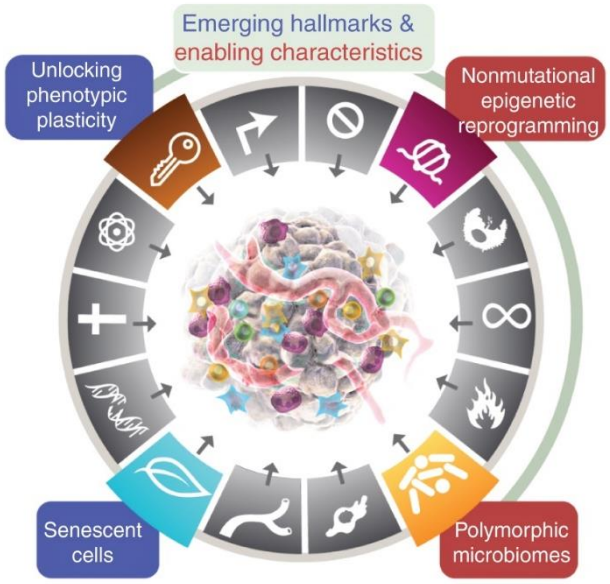

Figure 1.1 The Hallmarks of Cancer, circa 2022. (a) The ten hallmarks of cancer, **(b)** with the addition of two emerging hallmarks and enabling characteristics. Image is adapted from Hanahan, 2022 [HANAHAN, D. 2022. Hallmarks of Cancer: New Dimensions. *Cancer Discovery*, 12, 31-46, Figure 1, page 31].

1.2.2(b) Targeted therapy in CRC

Molecular targeted therapy is a therapeutic strategy that utilizes drugs to disrupt well-defined biological targets and pathways to achieve cancer cell regression and obliteration (Mocellin et al., 2005; Lee et al., 2018). The integration of molecular targeted therapy as the first-line treatment strategy in CRC was introduced and approved by FDA since the year 2004. Molecular targeted therapy in CRC can be characterized into three main approaches, by (1) targeting malignant cell-specific growth factors/receptors, (2) disruption of cancer pathways, and (3) suppression of tumour oncogenes.

1.2.2(b)(i) Targeting malignant cell-specific growth factors/receptors

Several targeted therapy agents, such as the monoclonal antibody-based drugs Cetuximab (Erbitux) and bevacizumab (Avastin) which target the epidermal growth factor receptors (EFGRs) and angiogenesis in CRC cells, have shown successful extension of CRC patient survivability (Seeber and Gastl, 2016; Xie et al., 2020). In addition, other EFGR- and vascular endothelial growth factor/receptor (VEGF/VEGFR)-targeting drugs such as Panitumumab (Vectibix), Ziv-aflibercept (Zaltrap), Ramucirumab (Cyramba), and Regorafenib (Stivarga) has also been approved by the FDA or EMA for use in CRC therapy. For metastatic CRC, immune checkpoint inhibitors including Pembrolizumab (Keytruda), Nivolumab (Opdivo), and Ipilimumab (Yervoy) are frequently employed as treatment options for patients with metastatic CRC (Xie et al., 2020; Seeber and Gastl, 2016).

1.2.2(b)(ii) Disruption of cancer pathways

In CRC, various cancer metastasis-contributing pathways such as the Wnt/β-catenin pathway, TGF-β/SMAD pathway, PI3K/AKT pathway, and RAS/RAF pathway are therapeutic targets of targeted therapy agents (Testa et al., 2020; Xie et al., 2020). Drug candidates targeting the Wnt pathway, such as the Frizzled 5 (FZD5) blocking peptide Foxy5 (WntResearch Ab), β-catenin inhibitor PRI-724 (Prism/Eisai pharmaceuticals), as well as porcupine inhibitors LGK974 (Novartis) and ETC159 (D3-Institute experimental therapeutics) are currently in development and under phase I, phase 1b, and phase I/II clinical trials for CRC treatment, respectively (Krishnamurthy and Kurzrock, 2018). Additionally, an anti-R-Spondin 3 antibody agent named OMP131R10 (Oncomed/Cell gene) is also under phase I clinical trial as an adjuvant for FOLFIRI in RSPO3 positive metastatic CRC (Krishnamurthy and Kurzrock, 2018). As the Notch pathway is highly implicated in CRC (Vinson et al., 2016b), a Gamma secretase inhibitor known as RO4929097 (Roche) was also developed and is under phase II clinical trial for the treatment of CRC (Krishnamurthy and Kurzrock, 2018).

1.2.2(b)(iii) Suppression of tumour oncogenes

Nevertheless, various targeted therapy agents have been developed to target cancer-specific mutations. Drugs such as Encorafenib (Braftovi) were used for the treatment of metastatic CRC harbouring the BRAF V600E mutation, while both Trastuzumab (Herceptin) and Lapatinib (Tykerb) were approved for the treatment of CRC with overexpressed HER2 gene (Ducreux et al., 2019; Shuford et al., 2020).

1.2.2(c) Limitations of targeted therapy in CRC

Overall, targeted therapies have shown beneficial outcomes in enhancing treatment efficacies and prolonging the survival of CRC patients (Jonker et al., 2007; Sartore-Bianchi et al., 2016; Overman et al., 2018). However, the application of targeted therapy agents as an adjunct to standard chemotherapy regimens failed to increase the PFS or OS rates of CRC patients significantly, despite showing the ability to improve clinical outcomes (Hurwitz et al., 2004; Tabernero et al., 2007; Van Cutsem et al., 2009b; Douillard et al., 2010; Maughan et al., 2011; Van Cutsem et al., 2012; Folprecht et al., 2016; Hong et al., 2016). One major challenge impeding the use of targeted therapies in the treatment of CRC is the genetic heterogenicity of CRC tumours, leading to acquired resistance toward currently available targeted therapy drugs. For instance, CRC and metastatic CRC harbouring RAS mutation were reported to exhibit poor response and/or develop resistance toward EGFR-targeted therapies and anti-angiogenic therapies (Di Fiore et al., 2007; Freeman et al., 2008; Zhao et al., 2017; Xie et al., 2020). Anti-EGFR therapies, anti-angiogenesis therapies, and immunotherapies were also associated with high toxicities, as evident via symptoms such as wound healing complications, mucosal bleeding, rashes, arterial thrombosis, cardiac dysfunction, organ inflammation and gastrointestinal perforation in post-treatment patients (Keefe and Bateman, 2019; Piawah and Venook, 2019). Several studies have also revealed the presence of severe synergistic toxicity effects in drug combinations involving multiple targeted therapy agents in patients from various types of cancers (Azad et al., 2008; Bitting et al., 2014; Ma et al., 2015; Postow et al., 2015; Xiao et al., 2015; Négrier et al., 2017; Keefe and Bateman, 2019); as well as substantial toxicities in CRC patients treated with a combination of targeted therapy agents and standard chemotherapy drugs (Folprecht et al., 2016).

1.2.3 Combination therapy in CRC

Palliative chemotherapy for advanced CRC includes 5-FU-based adjuvants such as FOLFOX (5-FU, leucovorin, and oxaliplatin) and FOLFORI (5-FU, leucovorin, and irinotecan) (Goldberg et al., 2004; Alberts et al., 2012; Cho et al., 2020; Xie et al., 2020). These combination treatments have greatly improved the patient response rate (Gu et al., 2019). However, 5-FU-based adjuvants especially FOLFOX were also found to be effective only toward early-stage CRC, but have limited benefits in improving the OS rate of stage II and stage III CRC patients (André et al., 2004). In addition, these chemotherapy combinations often increased the risk of CRC patients to grade 3 and grade 4 toxicities (Douillard et al., 2000; Porschen et al., 2001; Souglakos et al., 2006; Falcone et al., 2007). Therefore, adjuvant therapy was ascertained as an alternative treatment strategy to overcome chemotherapy-associated limitations in CRC. Although adjuvant therapy would aim to supplement post-surgical procedures by eradicating residual malignant cells to avoid disease recurrence, yet this treatment failed to improve the survival rate of late-stage CRC patients. Chemotherapy regimens for stage IV CRC cancer include 5-FU-leucovorin, FOLFOX, and FOLFIRI (Carethers, 2008b). Targeted therapy drugs that inhibit specific growth factors, such as bevacizumab (VEGF inhibitor) and cetuximab (EGFR inhibitor), were shown to enhance tumour shrinkage and increased OS of stage IV patients when supplemented with 5-FU-based regimens (Hurwitz et al., 2004; Jonker et al., 2007). The summary of FDA-approved drugs used in combination treatment for CRC is tabulated in Table 1.4.

Table 1.4 Summary of FDA-approved drugs used in combination treatment for CRC.

Drug	Single/ combination treatment	Success/ failure in clinical trials	References
Bevacizumab	Single	The overall incidence of FAEs with bevacizumab was 2.5% of total trial participants (10,216 patients), compared with 1.7 per cent of patients who did not. Therefore, treatment increased FAEs risk by approximately 50%.	(National Cancer Institute, 2011; Ranpura et al., 2011)
	Carboplatin and paclitaxel	FAEs risk was increased by more than three-fold compared to a single treatment.	
	IFL	Increased median OS of patients by 4.7 months with improved PFS rate.	
	FOLFOX4	Increased OS of patients by 2.2 months with improved PFS rate.	
Ramucirumab	FOLFIRI	Median overall survival was 13·3 months (536 patients).	(Tabernero et al., 2015)
Cetuximab	Single	The RR of patients with mutated KRAS was 0% whereas the RR of patients with wild-type KRAS was 40% (n=65). The PFS and OS of patients without KRAS mutation were significantly longer compared with patients harboring mutated KRAS (median PFS of 31.4 versus 10.1 weeks; median OS of 14.3 versus 10.1 months, respectively).	(Lièvre et al., 2008)
	Capecitabine and oxaliplatin	Addition of cetuximab to chemotherapy did not improve the OS of patients harbouring tumours expressing wild-type KRAS. The median survival time was 17.9 months in those treated with chemotherapy alone and 17.0 months in those treated with cetuximab plus chemotherapy. ORR increased from 57% (n=209) with chemotherapy alone to 64% (n=232) with addition of cetuximab (1630 patients). Increased skin irritations and gastrointestinal side effects of.	(Institute, 2011)

Table 1.4-1. Continued

		the chemotherapy drugs without improving patient survival	
	IFL	The hazard ratio for PFS in the cetuximab-FOLFIRI group as compared with the FOLFIRI group was 0.85. There was no significant difference in the OS rate between the two treatment groups. Reduced the risk of progression of metastatic colorectal cancer.	(Van Cutsem et al., 2009a)
Panitumumab	Single	No responders were identified in the panitumumab mutant KRAS group, whereas wild-type KRAS patients treated with panitumumab achieved a 17% ORR.	(Rodríguez et al., 2010)
	IFL or FOLFIRI	ORR was more than 40% and the disease control rate almost reached 80%.	
5-fluorouracil (5FU)	Leucovorin	The mainstay for the treatment of metastatic colorectal cancer. Increased ORR including a two-fold increase in tumour response rate in combination treatment (21%) compared to 5-FU alone (11%). The OS increased in patients treated with combination treatment (median survival of 11.7 months) versus 5-FU alone (median survival of 10.5 months).	(Thirion et al., 2004)
	Oxaliplatin	The 5-year DFS was significantly higher in the FOLFOX arm (73.3%) than in the 5-FU/LV monotherapy group (67.4%).	(Assed Bastos et al., 2010)
Capecitabine	Single	Provided advantages over administration of intravenous (IV) 5-FU plus leucovorin. Achieved a significantly superior tumour response rate (26% versus 17%), equivalent time to disease progression (4.6 versus 4.7 months), and equivalent OS (12.9 versus 12.8 months) when compared with results using 5-FU plus leucovorin (n=1207).	(Hirsch and Zafar, 2011)

Table 1.4-2. Continued

	Irinotecan hydrochloride	Increased RR by 50% and a disease control rate of 71%. With a median cohort follow-up of 30.5 months, the median time to progression and OS is 7.8 months and 16.8 months, respectively, in phase II trials.	(Patt et al., 2007)
	5-FU and leucovorin (5-FU/LV)	Compared to the Mayo Clinic regimen (FU and Calcium levofolinate), this combination regimen showed greater RR (25.8% versus 11.6%), median FFS (4.1 versus 3.1 months), and PFS (4.3 versus 4.7 months), and OS (12.5 versus 13.3 months), n=605.	(Comella, 2007)
Irinotecan hydrochloride	5-FU	Treatment-induced tumour shrinkage and improved patient survival by at least 2 months compared to 5-FU-leucovorin treatment alone.	(Saltz et al., 2000; Douillard et al., 2000)
	5-FU and leucovorin (5-FU/LV)	Increased the RR, and improved the PFS and OS of patients as compared with 5-FU/leucovorin single treatments. The combination of Irinotecan with 5-FU and leucovorin showed greater RR (39% versus 21%) and a significantly longer median PFS (7.0 versus 4.3 months) and OS (14.8 versus 12.6) compared to 5-FU/LV alone.	(Comella, 2007; Saltz et al., 2000)
Oxaliplatin	5-FU and leucovorin (LV5FU2)	Increased PFS (median of 9.0 versus 6.2 months) and better RR (50.7% versus 22.3%) compared to LV5FU2 alone.	(de Gramont et al., 2000)
		Combination treatment of Oxaliplatin with 5-FU and Leucovorin showed high RR in fluoropyrimidine-pre-treated patients with metastatic colorectal cancer, but the duration of response was relatively short. Overall RR was 42.0%, median response duration was 91 days and median duration of PFS was 132 days.	(Lee et al., 2001)

Table 1.4-3. Continued

	Capecitabine	No difference in RR (47% versus 49%), median PFS (7.0 vs 8.0 months) or OS (16.3 vs 17.2 months) compared to the combination treatment using FUFOX (5-FU and Oxaliplatin).	(Arkenau et al., 2005)

Abbreviations: FAE, fatal adverse effects; OS, overall survival, PFS, progression-free survival; KRAS, Kirsten rat sarcoma 2 viral oncogene homolog; EGFR, endothelial growth factor receptor; ORR, overall response rate; RR, response rate; DFS, disease-free survival; FFS, failure-free survival; IFL, combination treatment of irinotecan, fluorouracil and leucovorin (a.k.a. folinic acid); FOLFOX, combination treatment of folinic acid (a.k.a. leucovorin), fluorouracil and oxaliplatin; FOLFIRI, folinic acid, fluorouracil and irinotecan; FUFOX, fluorouracil/folinic acid and oxaliplatin.

1.3 The mammalian sirtuins (SIRTs)

SIRTs are class III histone deacetylases that are highly conserved and share a catalytic domain of ~275 amino acids with variable lengths of unique additional N-terminal and/or C-terminal sequences (Michan and Sinclair, 2007; Saunders and Verdin, 2007). The SIRT proteins utilize nicotinamide adenine dinucleotide (NAD^+) as a cofactor to sense oxidative, metabolic, or genotoxic stresses via detecting the fluctuation in cellular energies; which is crucial for the coordination of appropriate cellular responses (Imai et al., 2000; Alhazzazi et al., 2011). The SIRT proteins possess both lysine deacetylase and/or mono-ADP-ribosyltransferase enzymatic activities that target both histone and non-histone proteins (Saunders and Verdin, 2007; Martínez-Redondo and Vaquero, 2013). The seven members of the mammalian SIRT family (SIRT1-7) are known to vary in specificity, catalytic activity, substrates, and subcellular localization (Michan and Sinclair, 2007; Saunders and Verdin, 2007). Among all SIRTs, SIRT1 is prominently localized in the nucleus but also found in the cytosol; SIRT2 is present in the cytoplasm; SIRT3-5 is mainly mitochondrial; SIRT6 in the nucleus and SIRT7 in the nucleolus (Michan and Sinclair, 2007; Alhazzazi et al., 2011). Generally, SIRT functions can be classified into four main processes: chromatin regulation, cell survival under stress, metabolic homeostasis regulation, and developmental and cell differentiation (Bosch-Presegué and Vaquero, 2011). SIRTs are highly conserved enzymes implicated in many biological processes linked to longevity, ageing, DNA repair, epigenetic regulation, and metabolism homeostasis. Consequently, dysregulation of either one of these processes could result in tumorigenesis (Imai et al., 2000; Nakagawa and Guarente, 2011; Choi and Mostoslavsky, 2014; Carafa et al., 2019).

1.3.1 The roles of SIRTs in CRC

Increasing evidence has revealed the crucial role of SIRTs in cancer initiation and progression, and thus SIRTs have become the focus of increasing attention as potential targets in anticancer therapy (Saunders and Verdin, 2007; Bosch-Presegué and Vaquero, 2011; Carafa et al., 2012; Bosch-Presegue and Vaquero, 2014; Carafa et al., 2019). However, various reports also showed SIRTs to possess bifunctional and contradicting roles in cancer (Figure 1.2). In the events of cellular stress, the opposite roles of SIRTs can be exhibited, for instance, via the maintenance of DNA integrity (anti-tumour) versus the promotion of cell survival (pro-tumour). The roles and functions of each SIRTs in tumorigenesis and the development of CRC are discussed below.